Improved luminescent properties of $SrZn_2(PO_4)_2$:Sm^{3+} doped with Li^+, Na^+ and K^+ ions*

LU Wei (陆伟)[1], **LIU Yu-fei** (刘宇飞)[2], **WANG Ying** (王颖)[3], **WANG Zhi-jun** (王志军)[3]**, and PANG Li-bin** (庞立斌)[3,4]**

1. Tangshan Vocational & Technical College, Tangshan 063000, China

2. Library, Hebei University, Baoding 071002, China

3. College of Physics Science & Technology, Hebei University, Baoding 071002, China

4. Department of Foreign Language Teaching and Research, Hebei University, Baoding 071002, China

$SrZn_2(PO_4)_2$:Sm^{3+} phosphor was synthesized by a high temperature solid-state reaction in atmosphere. $SrZn_2(PO_4)_2$:Sm^{3+} phosphor is efficiently excited by ultraviolet (UV) and blue light, and the emission peaks are assigned to the transitions of $^4G_{5/2}$-$^6H_{5/2}$ (563 nm), $^4G_{5/2}$-$^6H_{7/2}$ (597 nm and 605 nm) and $^4G_{5/2}$-$^6H_{9/2}$ (644 nm and 653 nm). The emission intensities of $SrZn_2(PO_4)_2$:Sm^{3+} are influenced by Sm^{3+} concentration, and the concentration quenching effect of $SrZn_2(PO_4)_2$:Sm^{3+} is also observed. When doping A^+ (A=Li, Na and K) ions, the emission intensity of $SrZn_2(PO_4)_2$:Sm^{3+} can be obviously enhanced. The Commission Internationale de l'Eclairage (CIE) color coordinates of $SrZn_2(PO_4)_2$:Sm^{3+} locate in the orange-red region. The results indicate that the phosphor has a potential application in white light emitting diodes (LEDs).

In recent years, the key of developing white light emitting diodes (LEDs) is the red emitting phosphor that can improve the color rendering index of white LEDs[1]. Taking account of Sm^{3+} $^4G_{5/2}$-^6H_J emission in the red region, it is interesting to develop Sm^{3+} doped samples since such phosphors are expected to possess excellent red color purity[2]. Nevertheless, the low oscillator strength and narrow line width of Sm^{3+} 4f-4f absorption transitions will lead to a weak absorption in ultraviolet (UV) region, which leads to that Sm^{3+} doped phosphors present a weak orange-red or red emission. Therefore, it is necessary to find a method to enhance the emission intensity of Sm^{3+} doped phosphors[3]. Generally, luminescent materials consist of activator and host. In order to obtain efficient emission, the choice of host is another key factor, and the host must have excellent physical and chemical stability[4,5]. Among the compounds, phosphate is a good candidate due to the low cost, low synthetic temperature and good stability. For example, $MZn_2(PO_4)_2$ (M=Ca, Sr and Ba) has attracted extensive attention as host material for lanthanide activator[6-10]. However, there is no report about the luminescence of $SrZn_2(PO_4)_2$:Sm^{3+}. Hence, in this paper, Sm^{3+} doped $SrZn_2(PO_4)_2$ was synthesized, and its luminescent properties are improved by using A^+ (A=Li, Na and K) ions as compensator charge. The results may be useful for the development of red emitting phosphors.

Because of r_{Sm}≈0.108 nm, r_{Sr}≈0.112 nm and r_{Zn}≈0.074 nm, according to the effective ionic radii of cations with different coordination numbers, Sm^{3+} may preferably occupy Sr^{2+} sites in $SrZn_2(PO_4)_2$. A series of $Sr_{1-x}Zn_2(PO_4)_2$:xSm^{3+} and $Sr_{1-2x}Zn_2(PO_4)_2$:xSm^{3+}, xA^+ (A=Li, Na and K) were synthesized by a high temperature solid-state reaction. Initial materials (analytical grade) of $SrCO_3$, ZnO, $NH_4H_2PO_4$, Sm_2O_3, Li_2CO_3, Na_2CO_3 and K_2CO_3 were weighted in stoichiometric proportion, thoroughly mixed and ground by an agate mortar and pestle for more than 30 min till they were uniformly distributed. The mixed powders were calcined in corundum crucibles at 900 °C for 5 h in atmosphere. Finally, samples were cooled down to room temperature and ground thoroughly again into powders. Moreover, the samples were sieved under the same condition to ensure the similar particle size distribution.

Phase formation was determined by X-ray diffraction (XRD) in a Bruker AXS D8 advanced automatic diffractometer (Bruker Co., German) with Ni-filtered Cu Kα1 radiation (λ=0.154 06 nm), and a scan rate of 0.02°/s was applied to record the patterns in the 2θ range from 10° to

70°. Excitation and emission spectra were detected by a fluorescence spectrophotometer (Hitachi F-4600), and the exciting source was a 450 W Xe lamp. Commission International de I'Eclairage (CIE) chromaticity coordinates of phosphors were measured by a PMS-80 spectra analysis system. Each CIE chromaticity coordinate of samples is the average result of three times, and the accuracy is about 0.001. All measurements were carried out at room temperature.

For $Sr_{1-x}Zn_2(PO_4)_2$:xSm^{3+} and $Sr_{1-2x}Zn_2(PO_4)_2$:xSm^{3+}, xA^+ (*A*=Li, Na and K), a series of similar XRD patterns are observed for each sample. Fig.1 shows the XRD patterns of $SrZn_2(PO_4)_2$:$0.03Sm^{3+}$, $SrZn_2(PO_4)_2$:$0.03Sm^{3+}$, $0.03Li^+$, $SrZn_2(PO_4)_2$:$0.03Sm^{3+}$, $0.03Na^+$ and $SrZn_2(PO_4)_2$:$0.03Sm^{3+}$, $0.03K^+$. When comparing the diffraction data with the standard JCPDS card (No.80-1062), the results indicate that there is no difference between our samples and $SrZn_2(PO_4)_2$. The uniform diffraction pattern means that the phase formation of $SrZn_2(PO_4)_2$ is not influenced by a little Sm^{3+} and A^+. $SrZn_2(PO_4)_2$ monophosphate has monoclinic structure (space group: P2$_1$/c) with *a*=0.832 32 nm, *b*=0.951 01 nm, *c*=0.903 17 nm, *β*=92.293° and *z*=4.
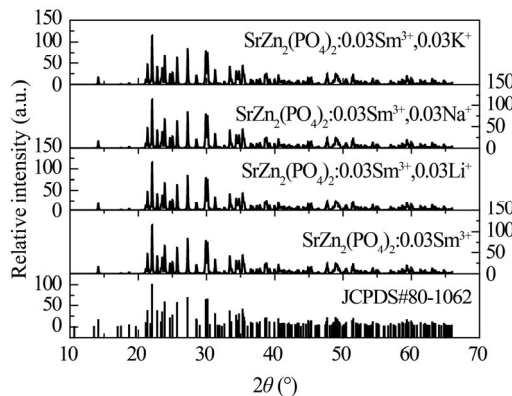
**Fig.1 XRD patterns of SrZn₂(PO₄)₂:0.03Sm³⁺ and SrZn₂(PO₄)₂:0.03Sm³⁺, A⁺ (A=Li, Na, K), compared with standard data of SrZn₂(PO₄)₂ (JCPDS No.80-1062)**

Fig.2 shows the spectral characteristics of $SrZn_2(PO_4)_2$:Sm^{3+}. For emission peak of 605 nm, the excitation spectrum has a series of peaks. Some peaks at 360 nm, 372 nm, 401 nm and 461 nm are ascribed to the transitions from the ground state to the excited states of Sm^{3+}. As shown in Fig.2 and Fig.3(a), among these excitation peaks, the strongest peak locates at 401 nm corresponding to the $^6H_{5/2}$-$^4K_{11/2}$ transition monitored at 605 nm. $SrZn_2(PO_4)_2$:Sm^{3+} exhibits several emission peaks, corresponding to the $^4G_{5/2}$-$^6H_{5/2}$ (563 nm), $^4G_{5/2}$-$^6H_{7/2}$ (597 nm and 605 nm) and $^4G_{5/2}$-$^6H_{9/2}$ (644 nm and 653 nm) transitions of Sm^{3+}[11]. Among these emission peaks, the red emitting transition is $^4G_{5/2}$-$^6H_{7/2}$ (597 nm and 605 nm), which satisfies the selection rule of $\Delta J=\pm1$, and it indicates that it is an allowed transition as a magnetic dipole (MD) but it is electric dipole (ED) dominated[11]. Therefore, it can be stated that it is partly MD and partly ED natured emission band. The other

transition of $^4G_{5/2}$-$^6H_{9/2}$ (644 nm and 653 nm) is purely an ED natured emission band, which is sensitive to the crystal field. Generally, the intensity ratio of ED and MD transitions can be used to understand the symmetry of the local environment of the trivalent 4f ions in the investigated host matrix. The larger the intensity of the ED transition, the more the asymmetric nature. In the present work, $^4G_{5/2}$-$^6H_{9/2}$ transition of Sm^{3+} ions is measured to be more intense than the MD transition of $^4G_{5/2}$-$^6H_{7/2}$, which describes the asymmetric nature of the investigated host.

In order to further optimize the red emission of Sm^{3+}, the concentration dependent emission intensity of $Sr_{1-x}Zn_2(PO_4)_2$:xSm^{3+} (*x*=0.005, 0.01, 0.02, 0.03, 0.04, 0.05, 0.07 and 0.10) is studied. The inset of Fig.2 shows that the emission intensity of $Sr_{1-x}Zn_2(PO_4)_2$:xSm^{3+} enhances with the increase of Sm^{3+} concentration, reaches its maximum value when Sm^{3+} concentration is *x*=0.03, and then decreases because of the concentration quenching effect. As shown in Fig.3(b), it may be ascribed to the presence of cross-relaxation between Sm^{3+} ions, and this process should be $^4G_{5/2}+^6H_{5/2}\rightarrow^6F_{9/2}+^6F_{9/2}$ between two adjacent Sm^{3+} ions[12].
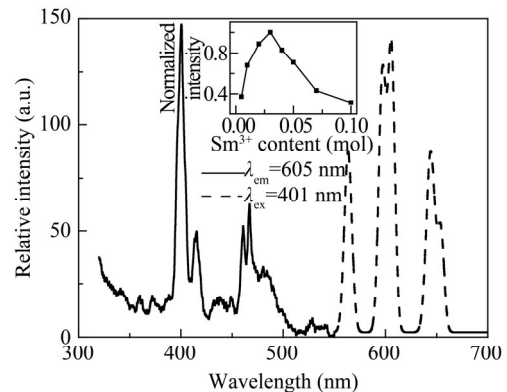
Fig.2 Emission and excitation spectra of SrZn₂(PO₄)₂: 0.03Sm³⁺ with λₑₓ=401 nm and λₑₘ=605 nm, respectively (The inset shows the emission intensity of SrZn₂(PO₄)₂: xSm³⁺ as a function of Sm³⁺ concentration with λₑₓ=401 nm.)
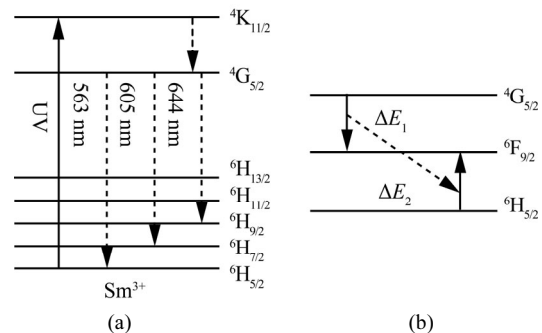
Fig.3 (a) ⁴G₅/₂→⁶H_{J/2} (J=5, 7 and 9) transitions of Sm³⁺; (b) Cross-relaxation process

As shown in the inset of Fig.2, the increase of emis-

sion intensity with low Sm^{3+} concentration ($x<0.03$) can be attributed to the large distance between Sm^{3+} ions, and then the emission intensity decreases which is possibly due to nonradiative energy transfer between Sm^{3+} ions. It is well known that the nonradiative energy transfer in the oxide is based on the resonance transfer by electric multipole-multipole interaction or exchange interaction. If the distance between activators is larger than the critical distance, the exchange interaction becomes ineffective, and only the multipolar interaction is important[13]. Thus, it is necessary to obtain the critical distance (R_c) between activator and quenching site. According to Ref.[13], R_c of energy transfer for $SrZn_2(PO_4)_2$:Sm^{3+} can be calculated by critical concentration of activator ion as

$$R_c \approx 2[3V/(4\pi x_c N)]^{1/3}, \qquad (1)$$

where x is the concentration of Sm^{3+}, N is the number of Z ions in the unit cell ($N=4$ for $SrZn_2(PO_4)_2$), and V is the volume of the unit cell ($V \approx 0.714\ 9\ nm^3$). In this case, the critical doping content of Sm^{3+} in $SrZn_2(PO_4)_2$ is 0.03 as shown in the inset of Fig.2. As a result, the R_c value of Sm^{3+} in $SrZn_2(PO_4)_2$ is approximately 1.123 nm. It means that the exchange interaction plays no role in the energy transfer between Sm^{3+} ions in $SrZn_2(PO_4)_2$. The radiation re-absorption comes into effect only when there is a broad overlap of fluorescent spectra of sensitizer and activator. However, its spectral characteristics show that it is unlikely to occur. So the multipolar interaction should be the major mechanism of concentration quenching for $SrZn_2(PO_4)_2$:Sm^{3+}. Dexter's theory proposed that the emission intensity per activator follows[14]

$$(I/x) = K[1+\beta(x)^{Q/3}]^{-1}, \qquad (2)$$

where x is activator concentration, $Q=6$, 8 and 10 for dipole-dipole (d-d), dipole-quadrupole (d-q), quadrupole-quadrupole (q-q) interactions, respectively, and for a given host crystal, K and β are constant for the same excitation conditions.

The critical concentration of Sm^{3+} has been determined to be 0.03. Fig.4 shows the plot of $log I/x_{Sm}^{3+}$ as a function of $log x_{Sm}^{3+}$ in $SrZn_2(PO_4)_2$:Sm^{3+}. It shows that the dependence of $log I/x_{Sm}^{3+}$ on $log x_{Sm}^{3+}$ is linear, and the slope is -2.02. The value of Q can be calculated as 6.06, which is about 6. It means that the d-d interaction is the concentration quenching mechanism of $SrZn_2(PO_4)_2$:Sm^{3+}.

The luminescent properties of phosphors arise from the complex interaction among host structure, activators, defects and interfaces. The charge unbalance and lattice distort can induce the point defects in the structure, which can increase the non-radiative process and then result in the reduction of emission intensity. For $SrZn_2(PO_4)_2$ host, Sm^{3+} ions enter the host crystal lattice and preferentially substitute for Sr^{2+} ions, which induces the charge unbalance. Alkali metal ions A^+ (A=Li, Na and K) may offset the charge unbalance generated by Sm^{3+} substitution for Sr^{2+}, reduce the lattice distortion, and enhance the luminescent intensity[15]. For $SrZn_2(PO_4)_2$:$0.03Sm^{3+}$, $0.03A^+$

phosphors, two Sr^{2+} ions are substituted by one Sm^{3+} and one A^+, which can be expressed as $2Sr_{Sr}^x \rightarrow Sm_{Sm}^\bullet + A_{Sm}'$.
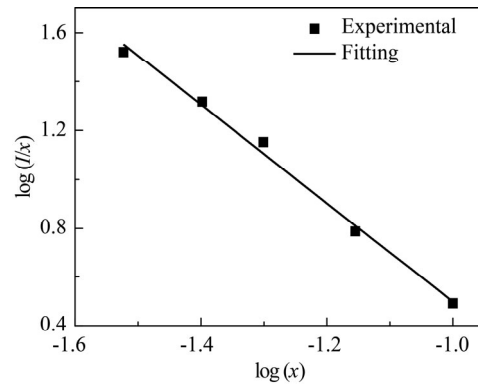
Fig.4 Plot of log(I/x) as a function of log(x) in SrZn$_2$(PO$_4$)$_2$:Sm^{3+}

Fig.5 shows the spectral properties of $SrZn_2(PO_4)_2$: $0.03Sm^{3+}$ and $SrZn_2(PO_4)_2$:$0.03Sm^{3+}$, $0.03A^+$ (A=Li, Na and K) phosphors. The emission intensities of $SrZn_2(PO_4)_2$: $0.03Sm^{3+}$, $0.03A^+$ are found to be stronger than that of $SrZn_2(PO_4)_2$:$0.03Sm^{3+}$, which indicates that A^+ ions can effectively enhance the emission intensity of $SrZn_2(PO_4)_2$: $0.03Sm^{3+}$. Moreover, Li^+ ion has the largest enhancement ability of efficient luminescence. Generally, the compensator charge with smaller radius can be easily incorporated into the host lattice. Therefore, Li^+ ion with $r_{Li} \approx 0.082$ nm may be the optimal selection for $SrZn_2(PO_4)_2$:Sm^{3+}.
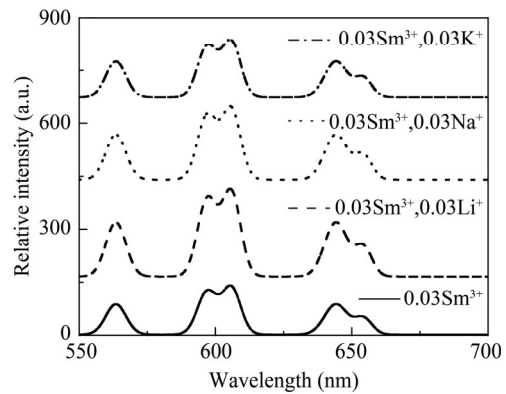
Fig.5 Emission spectra of SrZn$_2$(PO$_4$)$_2$:0.03Sm^{3+}, 0.03A^+ (A=Li, Na and K) (λ_{ex}=401 nm)

The color coordinate is one of the important factors for evaluating the performance of phosphor. The chromatic standard is issued by the Commission Internationale de l'Eclairage in 1931 (CIE 1931). The CIE chromaticity coordinates of $SrZn_2(PO_4)_2$:$0.03Sm^{3+}$ and $SrZn_2(PO_4)_2$: $0.03Sm^{3+}$, $0.03A^+$ (A=Li, Na and K) are shown in Tab.1, and the CIE chromaticity coordinates of phosphors have the similar values which all locate in the orange-red region.

Tab.1 CIE chromaticity coordinates of SrZn$_2$(PO$_4$)$_2$: 0.03Sm^{3+} and SrZn$_2$(PO$_4$)$_2$:0.03Sm^{3+}, 0.03*A*$^+$ (*A*=Li, Na and K)

Sample	CIE (x, y)
SrZn$_2$(PO$_4$)$_2$:0.03Sm^{3+}	(0.591 9, 0.320 3)
SrZn$_2$(PO$_4$)$_2$:0.03Sm^{3+}, 0.03Li$^+$	(0.591 7, 0.320 4)
SrZn$_2$(PO$_4$)$_2$:0.03Sm^{3+}, 0.03Na$^+$	(0.591 9, 0.320 5)
SrZn$_2$(PO$_4$)$_2$:0.03Sn^{3+}, 0.03K$^+$	(0.591 8, 0.320 4)

SrZn$_2$(PO$_4$)$_2$:Sm^{3+} was synthesized by the traditional solid-state method. SrZn$_2$(PO$_4$)$_2$:Sm^{3+} can create the orange-red emission under 401 nm excitation, and the peaks locate at 597 nm and 605 nm which are ascribed to ^{4}G$_{5/2}$-^{6}H$_{7/2}$ transition of Sm^{3+}. The excitation spectrum shows several excitation bands, and extends from 320 nm to 500 nm. The concentration quenching effect of SrZn$_2$(PO$_4$)$_2$:Sm^{3+} is observed, and the optimal concentration is 0.03. When doping *A*$^+$ (*A*=Li, Na, and K) as compensator charge, the emission intensities of SrZn$_2$(PO$_4$)$_2$:Sm^{3+} can be obviously enhanced, and the optimal candidate is Li$^+$. The CIE color coordinates of phosphors locate in the orange-red region. Therefore, SrZn$_2$(PO$_4$)$_2$:Sm^{3+} may have potential applications in white LEDs.

References

[1]   Li Jian, Deng Jia-chun, Lu Qi-fei and Wang Da-jian, Optoelectronics Letters **9**, 293 (2013).

[2]   WU Dong-ni, CUI Rui-rui and DENG Chao-yong, Journal of Optoelectronics·Laser **25**, 1516 (2014). (in Chinese)

[3]   Zhang Zhi-wei, Shen Xi-hai, Ren Yan-jun, Hou Wen-long, Zhang Wei-guo and Wang Dong-jun, Optics & Laser Technology **56**, 348 (2014).

[4]   WU Xia, Li Xu-cheng, LUO Si-yuan, GONG Xin-yong and DENG Chao-yong, Journal of Optoelectronics·Laser **24**, 2162 (2013). (in Chinese)

[5]   Zhang Zi-cai, Xu Shu-chao, Li Pan-lai, Wang Zhi-jun, Sun Jiang, Yang Zhi-ping and Pang Li-bin, Optoelectronics Letters **10**, 447 (2014).

[6]   Wang Zhijun, Li Panlai, Yang Zhiping and Guo Qinglin, Journal of Luminescence **132**, 1944 (2012).

[7]   Yi Linghong, Zhou Liya, Gong Fuzhong, Lan Yuwei, Tong Zhangfa and Sun Jianhua, Materials Science and Engineering: B **172**, 132 (2010).

[8]   Yang Woan-Jen and Chen Teng-Ming, Applied Physics Letters **88**, 101903 (2006).

[9]   Ding Haiyan, Huang Yanlin, Wei Donglei, Shi Liang, Qiao Xuebin and Seo Hyo Jin, Journal of The Electrochemical Society **156**, J312 (2009).

[10] Li Panlai, Wang Zhijun, Yang Zhiping and Guo Qinglin, Journal of Solid State Chemistry **220**, 227 (2014).

[11] Bandi V. R., Grandhe B. K., Jayasimhadri M., Jang K., Lee H.-S., Yi S.-S. and Jeong J.-H., Journal of Crystal Growth **326**,120 (2011).

[12] Wu Li, Ji Minyuan, Wang Hongrun, Kong Yongfa and Zhang Yi, Optical Materials Express **4**, 1535 (2014).

[13] Blasse G., Philips Res. Rep. **24**, 131 (1969).

[14] Van Uitert L. G., Journal of Electrochemical Society **114**, 1048 (1967).

[15] Xiao Quanlan, Dong Guoping and Qiu Jianrong, Journal of Luminescence **147**, 163 (2014).